Amide-Proton Exchange of Water-Soluble Proteins of Different Structural Classes Studied at the Submolecular Level by Infrared Spectroscopy †

ARTICLE *in* BIOCHEMISTRY · DECEMBER 1997

Impact Factor: 3.02 · DOI: 10.1021/bi971337p · Source: PubMed

3 AUTHORS:

Harmen H J de Jongh
TI Food and Nutrition
145 PUBLICATIONS **3,319** CITATIONS
SEE PROFILE

Erik Goormaghtigh
Université Libre de Bruxelles
170 PUBLICATIONS **5,717** CITATIONS
SEE PROFILE

Jean-Marie Ruysschaert
Université Libre de Bruxelles
472 PUBLICATIONS **13,911** CITATIONS
SEE PROFILE

Amide-Proton Exchange of Water-Soluble Proteins of Different Structural Classes Studied at the Submolecular Level by Infrared Spectroscopy[†]

Harmen H. J. de Jongh,[‡] Erik Goormaghtigh,* and Jean-Marie Ruysschaert

Laboratoire de Chimie-Physique des Macromolécules aux Interfaces, Université Libre de Bruxelles, CP 206/2, Boulevardd du Triomphe, B-1050 Bruxelles, Belgium

Received June 5, 1997; Revised Manuscript Received August 26, 1997[⊗]

ABSTRACT: For eleven films of various water-soluble α-, *β*-, α-/*β*-, and α-+*β*-proteins, the amide-proton exchange, initiated by exposure of the protein film to ^2H_2O, has been monitored using infrared spectroscopy. The approach to obtain the kinetics of exchange for four different classes of amide protons, correlating to the different secondary structure types, has been described in detail in the preceding paper. In this work the more general applicability of the approach is illustrated by testing it for different types of proteins. The results obtained are shown not only to be comparable to reported time-resolved nuclear magnetic resonance data (as in the case of myoglobin, phospholipase A_2, lysozyme, and cytochrome *c*), or to the more qualitative data obtained by neutron diffraction (trypsin, ribonuclease S, papain, and subtilisin BPN′), but the infrared approach us also provides with quantitative detailed insight on the distribution of exchange rate constants at the submolecular level of proteins, too complex to be studied by other techniques, as for tetrameric hemoglobin, and of proteins in which exchange is too fast to be detected by these other techniques, as is shown in this work for α-casein and apocytochrome *c*.

The study of hydrogen exchange of amide-protons with ^2H_2O has become increasingly important as a mean of characterizing the structure and dynamics of proteins. The measurement of hydrogen exchange is nonperturbing and can provide site-resolved information. Also the increasing understanding of the chemical and physical mechanisms underlying the exchange process (Englander & Kallenbach, 1984; Miller & Dill, 1995) makes this approach promising for the broad field of protein research. The approach has been applied to an increasing number of different techniques to gather information on a molecular level, such as infrared (IR)[1] (Goormaghtigh et al., 1994a; de Jongh et al., 1995), Raman (Hildebrandt et al., 1993), and mass (Robinson et al., 1994) spectroscopy. For a more resolved level, NMR (Wagner & Wüthrich, 1982; Zhang et al., 1995) or neutron diffraction (Kossiakoff, 1982) techniques have been used. In the preceding paper (de Jongh et al., 1997) we presented an IR approach enabling one to resolve the amide-protein exchange, in the case of bovine pancreatic trypsin inhibitor, in four classes corresponding to the four main secondary structures: α-helix, *β*-strand, *β*-turn, and random coil. In that work, the intensity changes at different wavenumbers within the amide I region, reflecting four different classes of exchange, were followed as a function of time of exposure of the protein to ^2H_2O. A good correlation between these classes and the different secondary structure types was found. The major advantage of this IR approach are, that time-resolved information can be obtained, suitable for a quantitative analysis, and that even at neutral pH's the exchange of solvent-exposed amides (at a second time scale) can be detected (Goormaghtigh et al., 1996).

The aim of this work is to demonstrate the more general applicability of this IR approach to monitor amide-proton exchange by applying it to a variety of water-soluble proteins from different structural classes and compare the results with NMR and neutron diffraction data when available in literature. The good correlation of the IR results to data obtained by other techniques and the small quantities of material required, together with the advantages mentioned above, make this approach a good alternative for existing methods to gain insight in stabilities of proteins at the level of secondary structures, especially of those proteins for which this information is not easy accessible by other techniques due to their complexity.

MATERIALS AND METHODS

Protein Purification. Sperm whale skeletal muscle myoglobin, bovine blood hemoglobin, bovine pancreatic ribonuclease S, bovine milk α-casein, horse heart cytochrome *c*, porcine pancreatic phospholipase A_2, chicken egg white lysozyme, papain (Papaya Latex, type IV), and subtilisin BPN′ (Nargase, type VII) were all obtained from Sigma (St. Louis, MO). Bovine pancreatic trypsin was obtained from Boehringer (Mannheim, Germany). Apocytochrome *c* was obtained by removal of the heme from cytochrome *c* as reported (Fisher et al., 1979). All proteins were purified from salts and other low molecular weight components by dissolving typically 20−25 mg of protein in 2 mL of 10 mM Tris (pH 6.6, HCl). The protein samples were loaded on a fast desalting column (PD-10 containing 9.1 mL of Sephadex-G25M, Pharmacia), pre-equilibrated with 10 mM Tris (pH 6.6, HCl), and eluted at 4 °C with 3 mL of the same buffer. Next, the proteins were dialyzed at 4 °C four times against 100 times excess triply distilled water. After lyophilization the proteins were stored at −20 °C. Weighed

[†] This work was supported by the Human Capital and Mobility Research Network of the European Commission (Grant No. CHRX-CT92-0018). E.G. is a Senior Research Associate of the National Fund for Scientific Research (Belgium).

* Correspondence should be addressed to this author. Tel: +32 2650 5386. FAX: +32 2650 5113.

[‡] Present address: Centre for Protein Technology (TNO-WAU), Bomenlaan 2, 6700 EV Wageningen, The Netherlands.

[⊗] Abstract published in *Advance ACS Abstracts,* October 15, 1997.

[1] Abbreviations: (ATR) FT-IR (attenuated total reflection) Fourier transform infrared; TSPA: 3-(trimethylsilyl)-$^2H_4$-propionic acid.

S0006-2960(97)01337-8 CCC: $14.00

amounts of proteins were dissolved (final concentration of 10 mg/mL) in 10 mM Tris buffer (pH 6.6) containing 25 mM 3-(trimethylsilyl)-$^2H_4$-propionic acid (TSPA) (Sigma, St. Louis, MO).

Preparation of Deuterated Proteins. To obtain proteins in which all labile protons are exchanged for deuterons, we dissolved typically 2 mg of protein in 150 mL of 10 M urea-d_4 [deuterated as described previously (de Jongh et al., 1992)] in ^2H_2O and incubated the sample for 24 h at room temperature. To remove the urea the sample was dialyzed 4 times against 34 times excess ^2H_2O at 4 °C, and the protein was subsequently lyophilized. Protein stock solutions of 10 mg/mL in 10 mM Tris buffer in ^2H_2O (pH 6.6) containing 25 mM TSPA were prepared, and stored at −20 °C until further use.

Infrared Measurements. Typically 20 μL protein stock solution (200 μg) were spread homogeneously on one side of a germanium crystal (50 × 20 × 2 mm, Harrick, Ossining NY) and dried by a N_2 gas flow. On top of the crystal a 1 mm spacer was placed and the crystal was covered by a stainless steel plate containing a gas inlet and an outlet, enabling one to expose the film to any experimental atmospheric condition. The crystal was placed under an aperture angle of 45°, yielding 25 internal reflections. Upon exposure of the film to a continuous flow of ^2H_2O-saturated N_2 gas (30 mL/min), spectra were recorded every 30 s during the first 10 min and next with exponentially increasing time intervals up to a total of 19 h of exposure, as described previously (de Jongh et al., 1995). All spectra were obtained at room temperature as averages of 16 or 32 scans (nominal resolution 2 cm^{-1}) using a Bruker IFS-55 spectrometer, equipped with a liquid nitrogen cooled mercury cadmium telluride detector in the 0−8000 cm^{-1} range with a nominal resolution of 1 cm^{-1}.

Analysis of Infrared Spectra. The digitalization of the spectra was enhanced to 0.5 cm^{-1} by zero-filling of the data prior to Fourier transformation. A full automatic procedure for spectral corrections for atmospheric water contributions and for the integration of various bands in the IR spectra was used, revealing integrals for the amide I (1704 ± 6 to 1600 ± 3 cm^{-1}), amide II (1600 ± 3 to 1496 ± 12 cm^{-1}), and amide II′ (1496 ± 5 to 1410 ± 10 cm^{-1}) as described previously (Goormaghtigh et al., 1994b; de Jongh et al., 1995). In this way also the integral of TSPA (855 ± 10 to 815 ± 10 cm^{-1}) was obtained. All intensities presented are relative to the averaged intensity in the 1800−1790 cm^{-1} region of the corresponding spectrum. The relative absorbance is defined as 103 times the detected absorbance, relative to the integral of the TSPA band at 835 cm^{-1}.

Laplace transformation of the data was performed using the algorithm as described in detail by Provencher (1982).

M*onitoring the Amide-Proton Exchange of Four Classes Correlated to the Different Secondary Structures.* The approach is based on monitoring the spectral changes in the amide I region (1700−1600 cm^{-1}) of protein IR spectra caused by the exchange of amide-protons for deuterons, as initiated by flushing the chamber to which the protein film is exposed with ^2H_2O-saturated N_2 gas. For a proper analysis of these intensities three other spectral changes in this spectral region are taken into account. These are intensity changes caused by (1) variation in the degree of hydration of the film (since the film thickness is directly related to the intensity observed), (2) replacement of residual H_2O (which has a strong absorption in the amide I region) by ^2H_2O, and (3) different spectral parameters for the side chains absorptions in the H_2O and ^2H_2O environment. For a complete description of these contributions and the correction procedures as applied to all data presented in this work, we refer to the preceding paper (de Jongh et al., 1997).

It has been described that upon hydrogen exchange the amide I band generally shifts 5−10 cm^{-1} to lower wavenumber [see for example Goormaghtigh et al. (1994b) for review]. Because peptide groups involved in different secondary structures absorb in distinct regions of the amide I (Susi et al., 1967; Timasheff et al., 1967), it can be expected that the time dependence of this shift differs throughout the amide I region, since each amide-proton exhibits a protection from exchange depending on the conformation it resides in. It was shown that, indeed, the kinetics of exchange of individual secondary structures could be followed by monitoring the intensity changes at different wavenumbers within the amide I as a function of time of exposure of the protein to ^2H_2O. As described in the preceding paper in detail, the shift to lower wavenumber of four classes of exchanging amide-protons can be monitored at 1656 cm^{-1} (class I + class II), 1620 cm^{-1} (class III) and at 1675 cm^{-1} (class III + class IV). The overlapping components at 1675 cm^{-1} are resolved by subtraction of the separately obtained kinetics of class III at 1620 cm^{-1}. The class II kinetics is monitored at the isobestic point of class I, generally found between 1653 and 1650.5 cm^{-1}. Because of the overlap of class I and class II in the 1660−1645 cm^{-1} region, spectra were deconvoluted using a Lorentzian function with a line width of 40 cm^{-1} followed by a Gaussian apodization function with a 20 cm^{-1} line width [for details see Goormaghtigh and Ruysschaert (1990)]. The isobestic point of the class I is searched by analyzing the first 10 min of the exchange kinetics. This defines the isobestic point for the fast exchanging amide protons only. Monitoring the intensity change at the isobestic point of class I reveals the exchange kinetic of class II alone. The advantage of using deconvoluted spectra is that the helical component in amide I is expected to be sharper than the disordered component (Chirgadze et al., 1973; Chirgadze & Braznikov, 1974; Venyaminov & Kalnin, 1991b). In turn, the helical component will be rather selectively further narrowed by the deconvolution procedure and thereby will be resolved over the broad disordered. Deconvoluted spectra were used only for the purpose of separating class I and class II components. All other analyses were performed on the original spectra.

The difference in the absolute magnitude of the intensity change recorded for each class for the non-deconvoluted spectra (before deuteration minus after complete amide-proton exchange) was used in an attempt to establish a correlation with the secondary structure content. The intensity changes were weighted by the molar absorptivities known for each secondary structure. The relative molar absorptivities were shown to be 1:0.69:0.33:0.38 for respectively β-strands:α-helices:β-turns:random coil (de Jongh et al., 1996). In agreement with usual assignments for the different secondary structure [for a review see Goormaghtigh et al. (1994c)], class I−IV are expected to correspond to disordered, helical, β-strand, and β-turn structures, respectively. The product of the total intensity change by the molar absobtivity was tentatively taken as the relative mole fraction of the secondary structure. For the details on these procedures and discussion of the assumptions involved we would like to refer to the preceding paper. A good correlation

between class I−IV and the contributions of respectively nonstructured, α-helical, β-stranded, and β-turn regions for this protein was shown in the preceding paper on trypsin inhibitor (de Jongh et al., 1997).

It must be noted that as far as the very fast exchanging class (class I) is concerned, two effects could modify the amide I band in addition to proton exchange: (1) formation of hydrogen bonds between water molecules and the carbonyl groups of the peptide backbone could produce the shift of the amide I band to lower wavenumber and (2) hydration-induced conformational changes can affect the band shape of the amide I band as revealed for some proteins upon lyophilization (hydration level below 0.04 g of water/g of protein) (Prestrelski et al., 1993). Our measurements could therefore, for class I, represent not only the exchange but a more general effect due to water accessibility to the protein backbone. Previously we have shown that protein films as prepared here have an average hydration level of 0.15−0.20 g of water per g of protein (de Jongh et al., 1996). Such a degree of hydration was shown to be sufficient to fulfil all hydrogen bonding requirements present in the native protein (Rupley et al., 1980). We therefore do not expect significant changes in hydrogen bonding between water molecules and the peptide backbone nor changes in the conformation of the protein which could affect the shape of amide I upon increasing the degree of hydration as might occur during the experiment.

RESULTS AND DISCUSSION

In the preceding paper we demonstrated that intensity changes in the amide I region monitored in the course of H/^{2}H exchange at various wavenumbers can be used to obtain information on the amide-proton exchange of individual classes correlated to the secondary structure types. In that study the amide-proton exchange of bovine pancreas trypsin inhibitor was studied as a test case and shown to be comparable to literature NMR data. In this work we will illustrate the more general applicability of the same approach by studying on the one hand a variety of proteins which amide-proton exchange has been reported in great detail, and on the other hand proteins whose complexity prohibits a detailed NMR or neutron diffraction analysis. First, the analysis of the amide-proton exchange of an α-protein (myoglobin) and a β-protein (trypsin) will be presented in more details as an illustration of the method for these types of proteins. Next, an overview of hydrogen exchange kinetics of several proteins belonging to different structural classes will be presented to illustrate the more general applicability and potentiality of this IR approach to study amide-proton exchange at a sub-molecular level.

Myoglobin. Figure 1 shows the amide I (1700−1600 cm^{-1}), amide II (1600−1500 cm^{-1}), and amide II′ (1500−1400 cm^{-1}) regions of IR spectra of a film of myoglobin exposed for different periods of time to N_2 gas saturated with ^2H_2O. It can be observed that upon exposure of the protein to ^2H_2O, the intensity of the amide II band decreases, whereas that of the amide II′ increases, both reflecting the exchange of all amide-protons present in the protein for deuterons. The amide I band is also affected by the exchange, showing a shift of the maximum of approximately 8 cm^{-1} to lower wavenumber (see inset Figure 1). The large spectral differences observed around 1680 cm^{-1} are mainly due to side chain contributions (arginine, asparagine, and glutamine)

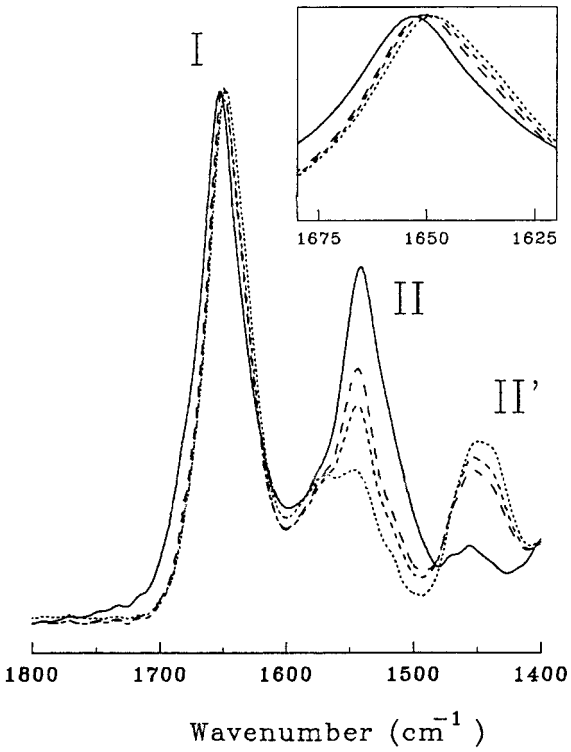

FIGURE 1: Infrared spectra of a film of 200 mg of myoglobin exposed for 0 min (—), 3 min (− −), 7 min (- - -), and 1120 min (···) to N_2 gas saturated with ^2H_2O as described in Materials and Methods. Indicated are the amide I, amide II, and amide II′ regions of the protein. The inset shows an expanded region of the amide I region. No TSPA was present in this sample.

that shift to the region around 1640 cm^{-1} upon changing from an H_2O to an ^2H_2O environment (Chirgadze et al., 1975; Venyaminov & Kalnin, 1991a). All of these intensity changes related to these side chain contributions are eliminated when analyzing the intensities at specific wavenumbers within amide I (see preceding paper).

Figure 2 shows the intensity at 1656 cm^{-1} (dashed line) upon exposure of a film of myoglobin to ^2H_2O. This kinetics can be resolved in two components (class I and class II) using the approach described before (isobestic point of class I exchange identified at 1650 cm^{-1}). The exchange kinetics of class II amides (open circles) shows two distinct phases; one exchanging rapidly within the first 15 min (approximately 45% of the total intensity change), but slower than observed for class I amides (closed circles), and a slow component that requires a few days to exchange completely. Since all intensity changes observed at 1656 cm^{-1} are defined to be determined by class I and class II only, it can be concluded from Figure 2 that the amide I contribution of class II is much larger than that of class I residues.

No significant intensity changes could be detected at 1675 and 1620 cm^{-1}, pointing to the absence of class III or IV amides in the protein. This also illustrates that the intensity changes in the 1680 cm^{-1} region (Figure 1) are indeed due to side chain contributions, since they have been eliminated completely during our analysis procedure.

The kinetics of exchange of the class I and class II contributions can be subjected to a Laplace transformation, as shown for myoglobin in Figure 3. In such an analysis the smallest number of rate constants required to describe the experimental data within the experimental accuracy margin is sought (Provencher, 1982). A clear discrimination between two components present in the class II (α-helical)

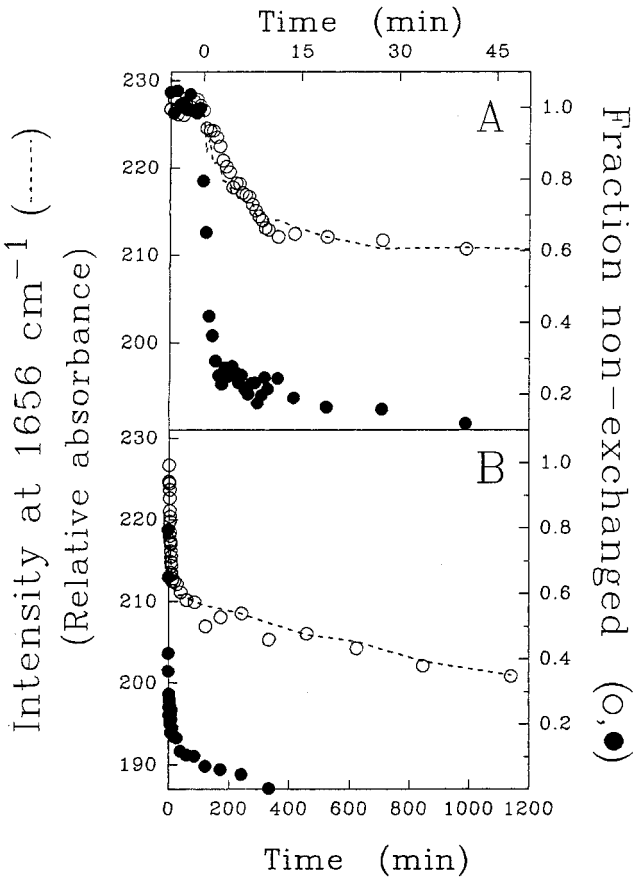

FIGURE 2: Intensity observed at 1656 cm^{-1} in IR spectra of a film of 200 mg of myoglobin containing 64 mg of TSPA is plotted as a function of time of exposure to ^2H_2O-saturated N_2 gas (left scale, dashed line). Also the fractions of non-exchanged amides assigned to class I (right scale, open circles) and those assigned to class II residues (right scale, solid circles) of myoglobin are plotted as a function of time of exposure. Panel A shows the time dependency prior to and during the first 50 min of exposure, whereas panel B displays the time span up to 19 h.

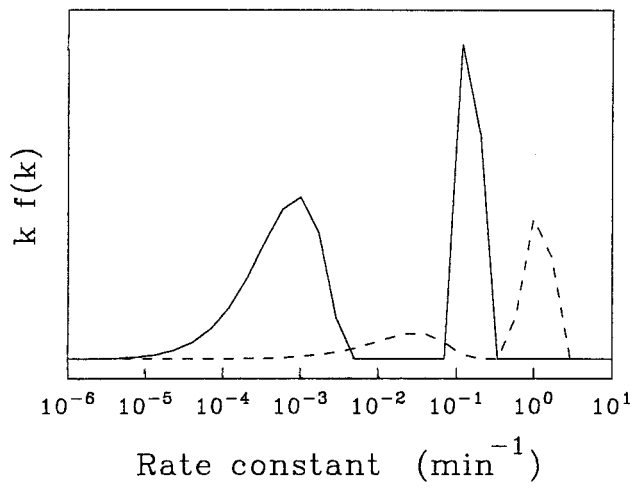

FIGURE 3: Distribution functions of the exchange rates of the class I (− −) and class II residues (—) of myoglobin upon exposure of a film of 200 mg of myoglobin containing 64 mg of TSPA to ^2H_2O-saturated N_2 gas. The distribution functions are obtained by a Laplace transformation of the exchange curves obtained for these classes. The intensities are scaled to the contributions of the secondary structure types present in myoglobin (see Table 1).

contribution can be seen. The fast exchanging component (45% of the integrated intensity of the distribution function) has exchange rates 200−250 times smaller than those present in the slow component. However, the majority of the class I (nonstructured) contribution exchanges still 10 times faster than the fast class II component.

From the total intensity differences of each of these classes before and after complete exchange of all amides, the secondary structure content can be evaluated when the reported molar absorptivities of the different secondary structures (de Jongh et al., 1996) are taken into account (see preceding paper for a detailed description of this procedure). These intensity differences and the calculated percentages secondary structure are shown in Table 1. It is found that myoglobin is mainly α-helical (71%) with some nonstructured parts (28%). The comparison of the exchange of the entire protein as a summation of the class I−IV contributions with the global exchange as monitored by the decrease of amide II or increase of the amide II′ integrated intensities, is shown in Figure 4. At the longer time scale a close agreement between these two data sets can be observed. However, within the first 10 min of the exchange some discrepancy appears (Figure 4A), which can be explained by the fact that no corrections for H_2O or side chain contributions have been made for the amide II′/I ratio, the intensities of which vary only within the first minutes of the exchange and result in an overestimation of the amide II′/I ratio. The general agreement between these two data sets indicates that all exchanging components have been detected by monitoring the kinetics at only a few positions within amide I, and that this IR approach could potentially be used to obtain insight on the secondary structure content of proteins.

The results on myoglobin obtained by our IR approach do agree well with the literature data, in which a helicity of approximately 70% of the residues has been reported (Kuriyan et al., 1986; Osapay et al., 1994), with approximately 40% having protection factors larger than 100 (Hughson et al., 1990), identified as residues in the so-called A, G, and H-helices.

Trypsin. As an example to illustrate the IR approach for a β-protein we choose to study the amide-proton exchange of bovine pancreatic trypsin, since its structure has been reported by NMR in detail (Perona et al., 1995) and its exchange behavior has been described qualitatively using neutron diffraction (Kossiakoff, 1982). When the intensity was monitored at the isobestic point of the class I amides (identified for this protein at 1650.5 cm^{-1}), no residual intensity change could be detected on a longer time scale of exposure of the protein to ^2H_2O, indicating the absence of class II contributions to the amide I. This was further confirmed by the observation that the kinetics of exchange of class I residues, determined by monitoring the intensity increase at 1640 cm^{-1}, accounted for all intensity losses observed at 1656 cm^{-1} during the exchange experiment (data not shown). The exchange kinetics of the class I (closed circles) exhibits a two-phase character (Figure 5A): 70% of class I exchanges rapidly (within 5 min), whereas the remaining 30% has a slower exchange that is complete in approximately 250 min (Figure 5B). The exchange kinetics of the class III (closed triangles) residues is also biphasic, with 40% exchanging within 10 min and 60% requiring at least 1200 min to exchange completely. Although class III residues could interfere with a proper analysis of the intensity a 1675 cm^{-1}, where intensity changes of both class III and IV are detected upon exchange, this latter component can be fully eliminated by a subtraction procedure as described in detail in the preceding paper. The exchange kinetics of

Table 1: Maximal Changes in Intensity at 1656 (Resolved in Class I/Nonstructured and Class II/α-Helix), 1620 cm^{-1} (Class III/β-Strands), and 1675 (Class IV/β-Turn) Expressed as the Relative Absorbance, Obtained by Comparison of IR Spectra before and after All Labile Protons Present in the Proteins are Replaced by Deuterium[a]

	class I/nonstructured	class II/α-helix	class III/β-strand	class IV/β-turn
myoglobin	7.3 (28%)	31.9 (71%)	−1.2 (1%)	0 (0%)
trypsin	19.5 (53%)	0 (0%)	−37.0 (38%)	3.0 (9%)
phospholipase A_2	11.2 (37%)	11.4 (38%)	−2.8 (9%)	5.0 (17%)
lysozyme	4.2 (17%)	10.7 (44%)	−4.6 (19%)	5.1 (21%)
papain	15.4 (33%)	20.7 (24%)	−39.0 (32%)	4.5 (11%)
ribonuclease S	14.3 (31%)	20.4 (24%)	−48.1 (40%)	2.0 (5%)
subtilisin BPN′	15.8 (43%)	16.3 (24%)	−21.1 (22%)	3.5 (11%)
cytochrome *c*	22.2 (53%)	29.4 (38%)	−1.1 (1%)	2.9 (8%)
hemoglobin	4.7 (12%)	61.3 (85%)	0 (0%)	2.5 (3%)
α-casein	16.5 (83%)	0 (0%)	−5.1 (10%)	1.2 (7%)
apocytochrome *c*	21.5 (87%)	0 (0%)	−6.5 (10%)	0.7 (3%)

[a] In brackets the secondary structure content is presented, calculated using the different molar absorptivities as reported previously for the different secondary structures (de Jongh et al., 1996).

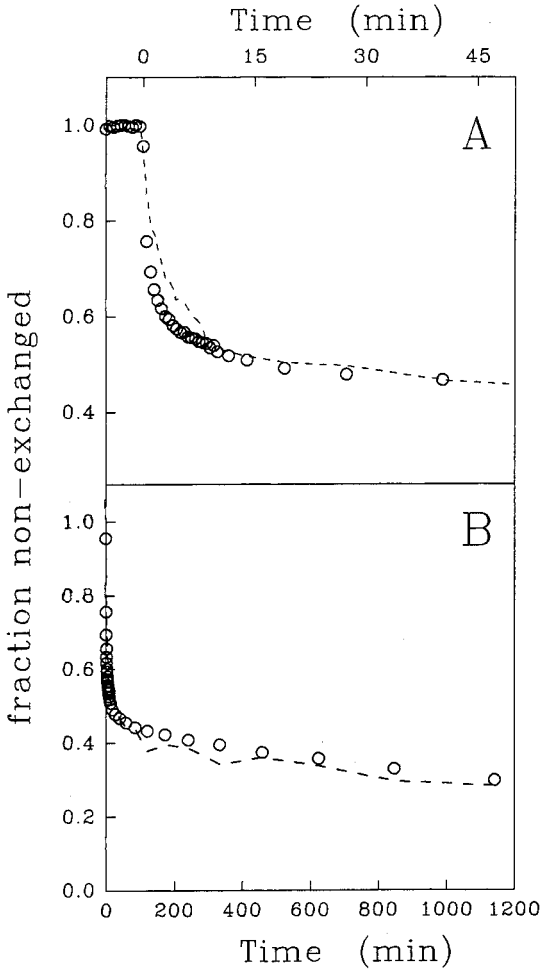

FIGURE 4: Sum of the contributions of the individual exchange kinetics secondary structure types present in myoglobin as shown in Figure 3 (○) and the normalized amide II′/I ratio (dashed line) observed for a film of 200 mg of myoglobin containing 64 mg of TSPA as a function of time of exposure to ^2H_2O-saturated N_2 gas.

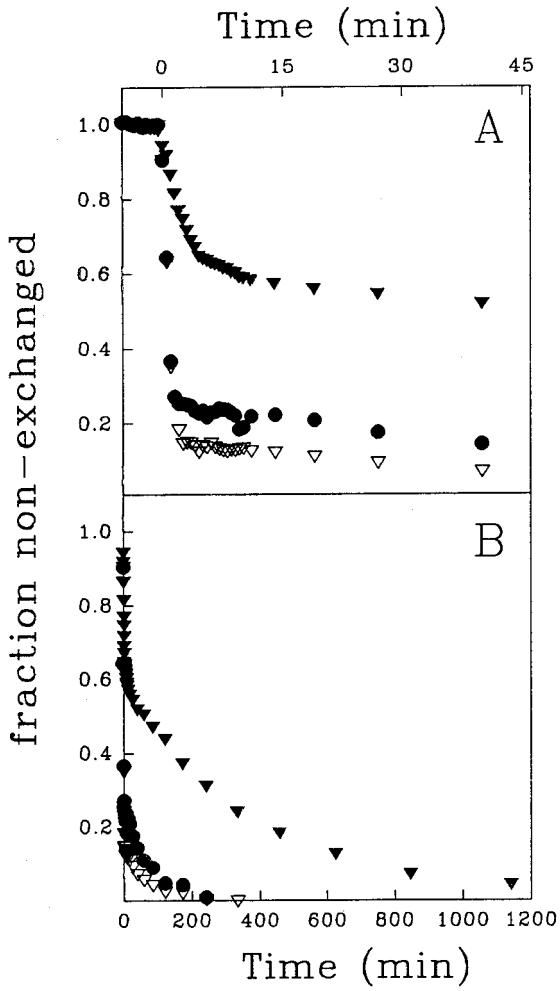

FIGURE 5: Fractions non-exchanged amides assigned to class I (●), class III residues (▼), and class IV (▽) are plotted as a function of time of exposure of a film of 200 mg of trypsin containing 64 mg of TSPA to ^2H_2O-saturated N_2 gas. Panel A shows the time dependency prior to and during the first 50 min of exposure, whereas panel B displays the time span up to 19 h.

class IV (open triangles) is completely distinct from that observed for class III residues, and resembling closely that of the class I amides of the protein. This illustrates that the intensity changes of the class III component in the 1680−1670 cm^{-1} region parallels that observed in the 1630−1620 cm^{-1} region. The maximal intensity changes before and after complete amide-proton exchange and the presumed calculated secondary structures content of trypsin are presented in Table 1. The summation of the kinetics obtained for the individual secondary structures multiplied by their fraction of presence in the protein, describes the normalized exchange curves obtained from the integrated intensity of amide II/I or amide II′/I well (data not shown), demonstrating again that the obtained kinetics for the various secondary structures account for all residues present in the entire protein

The Laplace transformations of the exchange kinetics of the various classes of residues present in trypsin are shown in Figure 6. These exchange rate distribution functions clearly display that, although the majority (60%) of the amides residing in class III (correlating to β-strands) are protected from exchange, some regions are easily accessible

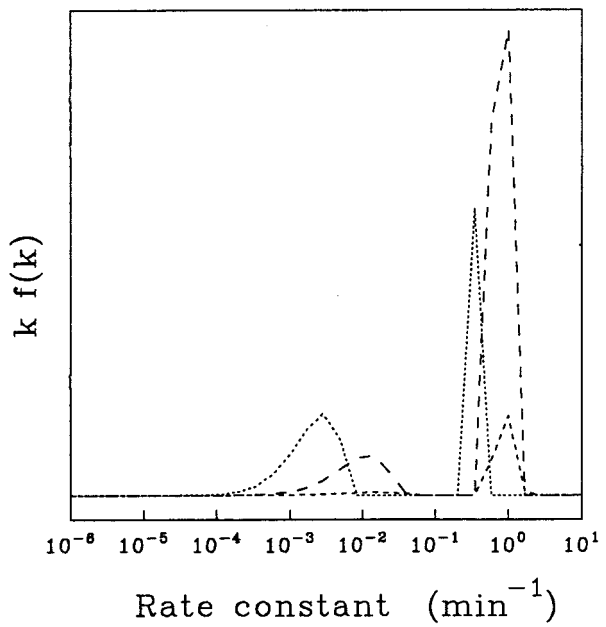

FIGURE 6: Distribution functions of the exchange rates of the class I (— —), class III (···), and class IV (- - -) of trypsin upon exposure of a film of 200 mg of trypsin containing 64 mg of TSPA to ^2H_2O-saturated N_2 gas. The distribution functions are obtained by Laplace transformation of the exchange curves obtained for these classes. The intensities are scaled to the contributions of the secondary structure types present in myoglobin (see Table 1).

to exchange with the solvent. Alternatively, the majority of the class I parts of the protein (assigned to nonstructured regions) offers no protection for their amides from exchange, and most likely reside at the outer surface of the protein. However, a significant number of residues (30%) belonging to class I are protected from exchange, and are possibly involved in hydrogen bonds or buried in the hydrophobic core of the protein. Interestingly, almost all class IV residues (β-turns) have exchange rates comparable to the fast exchanging component of class I residues.

From the qualitative exchange characteristics reported for the 223 residues of bovine pancreatic trypsin in a neutron diffraction study (Kossiakoff, 1982), it was concluded that 45 out of 91 β-stranded residues (50%) exchange very slowly whereas 8% of the β-residues have intermediate exchange rates. These numbers correspond closely to the 60% of the class III residues covered in the distribution function for the slow exchanging fraction (Figure 6), indicating again the good correlation between the defined classes and the secondary structure type they intend to represent. The neutron diffraction data also showed that at least seven residues with no regular structure had very slow exchange rates, whereas the rest exchanged too fast to be detected. Our studies indeed demonstrate a significant fraction of class I residues does show a protection from exchange.

Other Proteins. Figure 7 presents the amide-proton exchange rate distribution functions of the individual classes of the α-+β-proteins phospholipase A_2 (panel A), lysozyme (panel B), papain (panel C), and ribonuclease S (panel D); an α-/β-protein subtilisin BPN′ (panel E); the α-proteins cytochrome *c* (panel F) and hemoglobin (panel G); and the nonstructured proteins α-casein (panel H) and apocytochrome *c* (panel I). The estimated secondary structure contents as obtained from analysis of the maximal intensity changes in the amide I region before and after complete amide-proton exchange of these proteins are presented in Table 1.

Porcine pancreatic phospholipase A_2 (14 kDa) has a high structural stability due to seven internal disulfide bridges. The slow exchanging component of class II residues (±40%) observed by IR (Figure 7A) could correlate to the centers of the three helices present in this protein, whereas the faster component arises from residues at the ends of the helices, since the cores of the helices are reported to provide comparable protection from exchange as determined by NMR (Dekker et al., 1991). The β-stranded residues are known to be buried inside the protein (Dijkstra et al., 1983), providing a good protection from exchange, is indeed observed for the class III residues by IR (Figure 7A). The β-turns all face the solvent (Dijkstra et al., 1983), in agreement with the high exchange rates found for class IV here. When the exchange rates of the residues, as far as they could be determined by NMR (Dekker et al., 1991), are categorized per secondary structure and compared to the distribution functions as obtained by IR taking the pH difference into account, a close agreement can be found (not shown).

It has been reported that hen egg-white lysozyme (129 residues) has 48 amino acids in an α-helical conformation, of which 20 residues provide a strong, 15 an intermediate, and 13 a poor protection from exchange of their amides (Radford et al., 1992). Clearly, these three components can be discriminated from the class II exchange data obtained using the IR approach (Figure 7B), where the so-called A- and D-helix and the two 310 helices contribute most to the intermediate and fast exchanging component, whereas the B- and C-helices provide a strong protection from exchange. That the class III residues (representing the single β-strand in the protein) does provide less protection from exchange than the B- and C-helices, agrees very well with the literature (Radford et al., 1992), just as the observation that the loop regions (class IV) are all solvent exposed, resulting in fast exchange of their amides. Although the reported wavenumber for 310 helices is slightly different from that of a "regular" helix (Krimm & Bandekar, 1986), the present results suggest that it does not affect the analysis.

The exchange distribution functions of papain (212 residues) show that the majority of the class II and class III regions of the protein have very small exchange rate constants, whereas all other residues show almost no protection from exchange (Figure 7C). Obviously, the slow exchanging components are residues belonging to either a hydrophobic core known from X-ray studies to comprise three helices (so-called L-lobe), or to a second, even more hydrophobic, core made up by two helices and a distorted pleated β-sheet structure (Drenth et al., 1971). It is also known that one helix and a small proportion of the β-sheet, together with the turns present in the protein, are all located at a central groove, where the active site of the protein resides (Drenth et al., 1971; Pickersgill et al., 1992). Since a significant proportion of the class II, III, and IV amides of the protein do display a poor protection of its amides from exchange (Figure 7C), it can be suggested that in the absence of a substrate the region linking the two lobes is highly flexible. Such a flexible domain of the protein would be difficult to identify by NMR or X-ray techniques.

Only the amide-proton exchange of the S-peptide, the proteolytically cleaved amino-terminal 20 residues of ribonuclease A, has been reported in literature (Rashin, 1987). The exchange of the S-protein (residues 21−124), making up ribonuclease S when associated to the S-peptide, has never

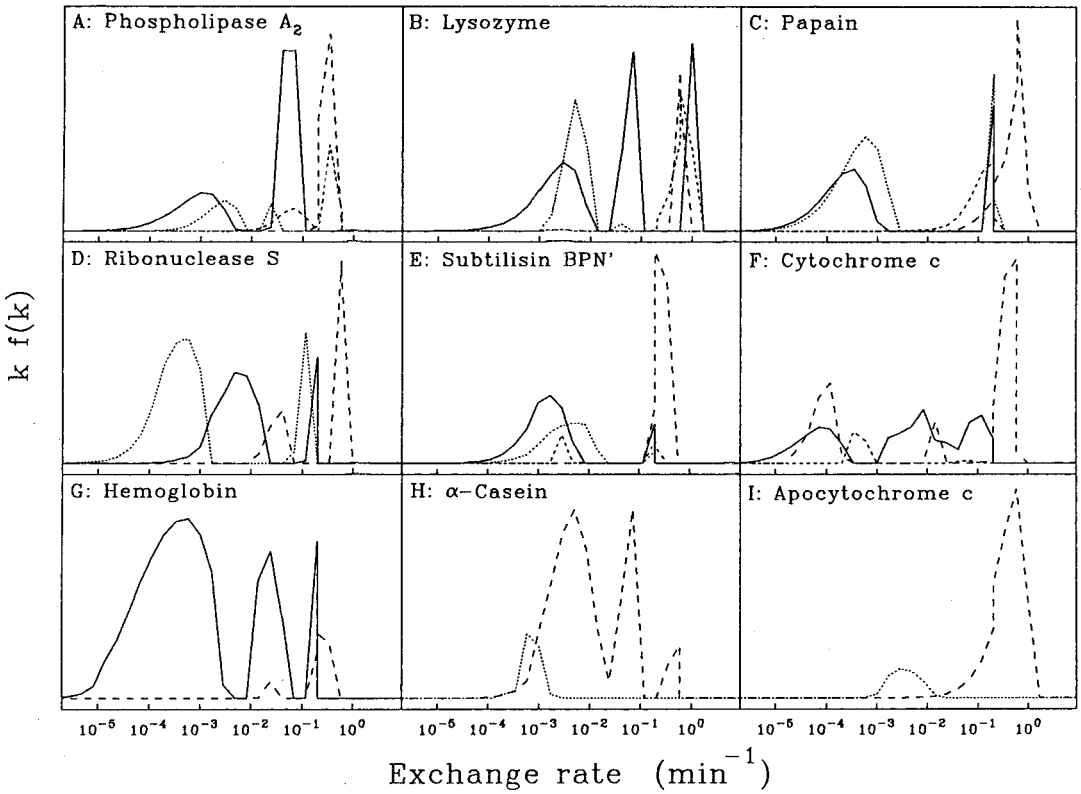

FIGURE 7: Distribution functions of the exchange rates of the class I (nonstructured; − −), class II (α-helical; —), class III (*β*-stranded; ···), and class IV (*β*-turns; - - -) residues of phospholipase A_2 (A), lysozyme (B), papain (C), ribonuclease S (D), subtilisin BPN′ (E), cytochrome *c* (F), hemoglobin (G), α-casein (H), and apocytochrome *c* (I) upon exposure of a film of 200 mg of protein containing 64 mg of TSPA to ^2H_2O-saturated N_2 gas, as detected by monitoring the intensities at different positions within the amide I region of IR spectra. The distribution functions are obtained by Laplace transformation of the exchange curves obtained for these classes. The intensities are scaled to the contributions of the secondary structure types present in myoglobin (see Table 1).

been reported, in contrast to that of the non-proteolytically cleaved protein (ribonuclease A). The maximal intensity change of class III could reflect 31% of the residues having a *β*-stranded conformation (Table 1), in agreement with the reported X-ray structure (Kim et al., 1992). The observation that the large majority of class III exchanges very slow (Figure 7D) is also in good agreement with qualitative data on the *β*-strands in ribonuclease A (Wlodawer & Sjîlnin, 1983). From this latter work it was also concluded that the helices [27% according to Kim and co-workers (1992)] were less stabilized, as confirmed by the characteristics of the class II exchange of our IR analysis.

It is interesting to observe that subtilisin BPN′, a protein (275 residues) with 5 α-helices and 7 *β*-strands in an alternating topological pattern, exhibits a small diversity in exchange rate constants for the class II, III and IV (Figure 7E). The majority of the class III residues exchange slowly, in agreement with qualitative neutron diffraction data of the *β*-stranded regions (Kossiakoff et al., 1991). Only a small proportion (<5%) of the class II amides exchanges fast (Figure 7E). This in contrast to a previous report where 21 out of the 73 helical residues showed a significant protection from exchange (Kossiakoff et al., 1991). This difference could be explained by the fact that when the isobestic point of the class I (nonstructured amides) is searched, the assumption is made that the class II (helical) amides have a general slower exchange behavior compared to those of class I domains. Consequently, class II residues, having no protection by their structure, are assigned during the discrimination procedure as class I residues. This results in an underestimation of the helical and overestimation of the nonstructured content in this IR approach (Table 1), as is indeed apparent upon comparison of our data with the reported X-ray structure (Polgar & Bender, 1969).

Whereas in all proteins discussed above the central core of the protein is dominated by a packing of secondary structure elements, in cytochrome *c* (104 amino acids) a heme group tightens the tertiary fold of the protein (Dickerson et al., 1971). From the amide-proton exchange data obtained by IR (Figure 7F) it can be seen that the class II (α-helical) residues have rate constants distributed over a broad range. Interestingly, 50% of the class I (nonstructured) amides show no protection from the solvent. The rest of these residues have exchange rates comparable to those obtained for the slowly exchanging component of the class II residues (around 10^{-4} min^{-1}). Some very slow exchange is also observed for some of the class IV residues. Comparison of the exchange rates of the different classes presented in Figure 7 with reported NMR data (Jeng et al., 1990) reveal close agreement between the intended secondary structure of a particular class and the NMR data classified per secondary structure element (data not shown).

The three-dimensional structure of myoglobin and the α- or *β*-chain of hemoglobin (a tetrahedral array of four chains of around 145 residues each) are quite similar, with heme groups located in crevices near the exterior of the protein. Interestingly, also their exchange rate constant distribution functions show a remarkable resemblance (compare Figure 3 with Figure 7G). Apparently, the tetrameric assembly does result in one striking difference: in hemoglobin an additional class II (helical) component is present with exchange rates around 2×10^{-2} min^{-1}, which could possibly arise from helices at the interface between the monomers.

Proteins known to lack any significant secondary structure, such as α-casein, can still display slow amide-proton exchange (Figure 7H). Demonstrated in Table 1 and reported previously (Jackson & Mantsch, 1991), α-casein is secondary nonstructured, but significant protection from exchange is observed for large parts of the protein. This could be caused by the strong association behavior of this protein to form micellar structures, as suggested previously (Markus et al., 1993). This in contrast to another nonstructured protein, apocytochrome *c*, that does show exchange kinetics where amides do have a fast exchange (completed in seconds), as detected by the IR approach (Figure 7I) and in agreement with previous reports on this protein (de Jongh et al., 1992).

For all proteins described above the summed exchange kinetics of the individual classes scaled to each other by the corresponding contribution to the entire protein (Table 1) was comparable to the kinetics obtained for the entire protein from the normalized amide II′/I ratio, indicating that in all cases no significant contribution of amides was not detected by the IR approach, and that the estimated secondary structure content was a good reflection of the apparent conformation of the protein (data not shown).

Summarizing, the IR approach enabling one to study the amide-proton exchange at the level of secondary structures, as presented in detail in the preceding paper, is shown in this work to be also applicable to eleven other water-soluble proteins from various structural classes. Not only is lThe information obtained on the exchange kinetics of the different structural classes comparable to that obtained by time-resolved NMR, as demonstrated in this work for myoglobin, phospholipase A_2, lysozyme, and cytochrome *c*, or to the more qualitatively data obtained with neutron diffraction, as shown for trypsin, papain, and subtilisin BPN′, it can also provide us with a quantitative detailed insight on the distribution of exchange rate constants of individual secondary structures present in proteins too complex to be studied by neutron diffraction or NMR (as the tetrameric hemoglobin), or proteins which exchange is too fast to be detected easily by these techniques (as for α-casein and apocytochrome *c*). Comparison of the secondary structures estimated using this IR approach (see Table 1) with the reported structures by other techniques, agrees generally within 5−10%. The results presented in this work prove the potentialities this IR approach might offer, in addition to the other established techniques, to be helpful for the characterization of the structure and dynamics of water-soluble proteins.

REFERENCES

Chirgadze, Y. N., & Brazhnikov, E. V. (1974) *Biopolymers 13*, 1701−1712.

Chirgadze, Y. N., Shestopalov, B. V., & Venyaminov, S. Y. (1973) *Biopolymers 12*, 1337−1351.

Chiradze, Y. N., Fedorov, O. V., & Trushina, N. P. (1975) *Biopolymers 14*, 679−694.

de Jongh, H. H. J., Killian, J. A., & de Kruijff, B. (1992) *Biochemistry 31*, 1636−1643.

de Jongh, H. H. J., Goormaghtigh, E., & Ruysschaert, J.-M. (1995) *Biochemistry 34*, 172−179.

de Jongh, H. H. J., Goormaghtigh, E., & Ruysschaert, J.-M. (1996) *Anal. Biochem. 242*, 95−103.

de Jongh, H. H. J., Goormaghtigh, E., & Ruysschaert, J.-M. (1997) *Biochemistry 36*, 13593−13602.

Dekker, N., Peters, A. R., Slotboom, A. J., Boelens, R., Kaptein, R., & de Haas, G. (1991) *Biochemistry 30*, 3135−3147.

Dickerson, R. E., Takano, T., Eisenberg, D., Kallai, O. B., Samson, L., Cooper, A., & Margoliash, E. (1971) *J. Biol. Chem. 246*, 1511−1535.

Dijkstra, B. W., Renetseder, R., Kalk, K. H., Hol, W. G. J., & Drenth, J. (1983) *J. Mol. Biol. 168*, 163−179.

Drenth, J., Jansonius, J. N., Koekoek, R., & Wolthen, B. G. (1971) *Adv. Protein Chem. 25*, 79−115.

Englander, S. W., & Kallenbach, N. R. (1984) *Q. Rev. Biophys. 16*, 521−655.

Fisher, W. R., Taniuchi, H., & Anfinsin, B. B. (1973) *J. Biol. Chem. 248*, 3188−3195.

Goormaghtigh, E., & Ruysschaert, J.-M. (1990) in *Molecular description of biological membranes by computer aided conformational analysis* (Brasseur, R., Ed.) Vol. 1, CRC Press Inc., Boca Raton, FL.

Goormaghtigh, E., Vigneron, L., Scarborough, G., & Ruyschaert, J.-M. (1994a) *J. Biol. Chem. 269*, 27409−27413.

Goormaghtigh, E., Cabiaux, V., & Ruysschaert, J.-M. (1994b) *Subcell. Biochem. 23*, 363−404.

Goormaghtigh, E., Cabiaux, V., & Ruysschaert, J.-M. (1994c) *Subcell. Biochem. 23*, 405−450.

Goormaghtigh, E., de Jongh, H. H. J., & Ruysschaert, J.-M. (1996) *Appl. Spectrosc. 50*, 1519−1527..

Hildebrandt, P., VanHecke, F., Heibel, G., & Mauk, A. G. (1993) *Biochemistry 34*, 14158−14164.

Hughson, F. M., Wright, P. E., & Baldwin, R. L. (1990) *Science 249*, 1544−1548.

Jackson, M., & Mantsch, H. M. (1991) *Biochim. Biophys. Acta 1078*, 231−235.

Jeng, M.-F., Englander, S. W., Elöve, G. A., Wand, A. J., & Roder, H. (1990) *Biochemistry 29*, 10433−10437.

Kim, E. E., Varadarajan, R., Wyckoff, H. W., & Richards, F. M. (1992) *Biochemistry 31*, 12304−12314.

Kossiakoff, A. A. (1982) *Nature 296*, 712−721.

Kossiakoff, A. A., Ultsch, M., White, S., & Eigenbrot, C. (1991) *Biochemistry 30*, 1211−1221.

Krimm, S., & Bandekar, J. (1986) *Adv. Protein Chem. 38*, 181−364.

Kuriyan, J., Wilz, S., Karplus, M., & Petsko, G. A. (1986) *J. Mol. Biol. 192*, 133−154.

Markus, G., Hitt, S., Harvey, S. R., & Tritsch, G. L. (1993) *Fibrinolysis 7*, 229−236.

Miller, D. W., & Dill, K. A. (1995) *Protein Sci. 4*, 1860−1873.

Osapay, K., Theriault, Y., Wright, P. E., & Case, D. A. (1994) *J. Mol. Biol. 244*, 183−197.

Perona, J. J., Hedstrom, L., Rutter, W. J., & Flettbrick, R. J., (1995) *Biochemistry 34*, 1489−1499.

Pickersgill, R. W., Harris, G. W., & Garman, E. (1992) *Acta Crystallogr. B 48*, 59−67.

Polgar, L., & Bender, M. (1969) *Proc. Natl. Acad. Sci. U.S.A. 64*, 1335−1342.

Provencher, S. W. (1982) *Comput. Phys. Commun. 27*, 213−227 and 229−242.

Radford, S. E., Buck, M., Topping, K. D., Dobson, C. M., & Evans, P. A. (1992) *Proteins: Struct., Funct., Genet. 14*, 237−248.

Rashin, A. A. (1987) *J. Mol. Biol. 198*, 339−350.

Robinson, C. V., Gross, M., Eyles, S. J., Ewbank, J. J., Mayhew, M., Hartl, F.-U., Dobson, C. M., & Radford, S. E. (1994) *Nature 372*, 646−651.

Rupley, J. A., Yang, P., & Tollin, G. (1980) in *Water in Polymers* (Rowland, S. O., Ed.), pp 111−132, American Chemical Society, Washington, DC.

Susi, H., Timasheff, S. N., & Stevens, L. (1967) *J. Biol. Chem. 242*, 5460−5466.

Timasheff, S. N., Susi, H., & Stevens, L. (1967) *J. Biol. Chem. 242*, 5467−5473.

Venyaminov, S. Y., & Kalnin, N. N. (1991a) *Biopolymers 30*, 1243−1257.

Venyaminov, S. Y., & Kalnin, N. N. (1991b) *Biopolymers 30*, 1259−1271.

Wagner, G., & Wüthrich, K. (1982) *J. Mol. Biol. 160*, 343−361.

Wlodawer, A., & Sjîlin, L. (1983) *Biochemistry 22*, 2720−2728.

Zhang, Y. Z., Paterson, Y., & Roder, H. (1995) *Protein Sci. 4*, 804−814.

BI971337P